ACS Macro Letters

Letter

pubs.acs.org/macroletters

In-Depth Profiling of Degradation Processes in a Fuel Cell: 2D Spectral-Spatial FTIR Spectra of Nafion Membranes

Marek Danilczuk,[†] Lukasz Lancucki,[†,‡] Shulamith Schlick,*[,†] Steven J. Hamrock,[§] and Gregory M. Haugen[§]

[†]Department of Chemistry and Biochemistry, University of Detroit Mercy, 4001 West McNichols Road, Detroit, Michigan 48221, United States

[§]3M Fuel Cell Components Group, 3M Center, St. Paul, Minnesota 55144, United States

Supporting Information

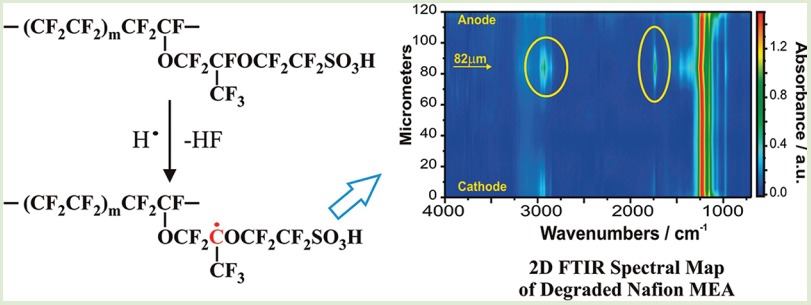

ABSTRACT: We present in-depth profiling by micro FTIR of cross sections for Nafion 115 membranes in membrane-electrode assemblies (MEAs) degraded during 52 or 180 h at open circuit voltage (OCV) conditions, 90 °C and 30% relative humidity. Analysis of optical images showed highly degraded zones in both MEAs. Corresponding 2D FTIR spectral-spatial maps indicated that C−H and C═O groups are generated during degradation. The highest band intensities for both groups appeared at a depth of 82 μm from the cathode in the MEA degraded for 180 h; the same bands were present but less intense at a depth of 22 μm from the cathode. Degradation at these depths is most likely associated with the location of the Pt band formed from Pt dissolution and migration into the membrane. The two degradation bands, C═O and C−H, appeared at the same depths from the cathode, 82 and 22 μm, suggesting that they are generated by a common mechanism or intermediate. This result is rationalized by a very important first reaction: Abstraction of a fluorine atom from the polymer main chain and side chain by hydrogen atoms, H$^{\bullet}$. This step is expected to cause main chain and side chain scission and to generate R_F−$CF_2^{\bullet}$ radicals that can react with H_2O_2, H_2O, and H_2 to produce both −COOH and RCF_2H groups.

Proton exchange membrane fuel cells (PEMFCs), which convert the chemical energy from the reaction of hydrogen and oxygen to electrical energy, are a promising source of clean energy for stationary, portable, and automotive applications. Important components of a FC are the catalyst, the proton exchange membrane (PEM), and the fuel (hydrogen or, in some cases, methanol). The role of the membrane is crucial: To separate the cathode and anode compartments and to allow efficient proton transport from the anode to the cathode.[1] Current active research is focused on understanding the mechanism of membrane degradation, and on methods of membrane stabilization by mitigating cations such as Ce(III) and Mn(II).[2]

Many studies have centered on the behavior of perfluorinated membranes such as Nafion, Aquivion (a Solvay-Solexis product), and the 3M membrane available from the 3M Company, because of their superior chemical, mechanical, and thermal stability; however, in all cases, the membrane lifetime is limited by the highly reactive species present in an operating PEMFC. A well-documented and widely accepted degradation mechanism is attack of hydroxyl radicals, HO$^{\bullet}$, on residual −COOH end groups in the polymer *backbone*, leading to the unzipping mechanism.[3] The proposed steps of this process are:

$$R_F{-}CF_2COOH + HO^{\bullet} \rightarrow R_F - CF_2^{\bullet} + CO_2 + H_2O$$

$$R_F{-}CF_2^{\bullet} + HO^{\bullet} \rightarrow R_F{-}CF_2OH$$

$$R_F{-}CF_2OH \rightarrow R_F{-}COF + HF$$

$$R_F{-}COF + H_2O \rightarrow R_F{-}CF_2COOH + HF$$

However, major ideas on the degradation mechanism in perfluorinated ionomers have undergone significant modifications in the past few years. Recent studies have emphasized the susceptibility of the ionomer *side chains* to chemical attack,[4] a process that becomes even more important in chemically

Received: September 29, 2011
Accepted: January 3, 2012
Published: January 13, 2012

stabilized membranes in which the amount of the −COOH end groups is reduced by processes such as exposure to molecular fluorine.[5] Schiraldi et al. have used low molecular weight model compounds to study the mechanism of chemical degradation of perfluorinated and hydrocarbon-based membranes. The results clearly showed that degradation is initiated by radical attack on the polymer backbone carboxylic acid groups and on the side chain in fluorinated PEM materials. In hydrocarbon systems, the aromatic groups can be hydroxylated, leading to chain scission.[5]

We have developed direct electron spin resonance (ESR)[4] and spin trapping ESR studies[6] for the study of membrane degradation. These studies have suggested that the hydroxyl radical, $HO^{\bullet}$, is an aggressive oxygen radical that may attack both the main and side chains in PEMs; examined the difference between ex situ experiments on model compounds and membranes and in situ experiments in a PEMFC inserted in the ESR resonator; and developed methods for the detection of early events and for identification of unstable intermediates.[6] The important role of $HO^{\bullet}$ has been reinforced by an analysis of the mitigating effect of Ce(III).[6c] The presence of hydrogen atoms, $H^{\bullet}$, has been detected for the first time in our study of Nafion fragmentation in a PEMFC inserted in the resonator of the ESR spectrometer.[6b] During in situ experiments, the presence of adducts of the spin trap 5,5-dimethyl-1-pyrroline *N*-oxide (DMPO) were identified: the DMPO/OOH adduct was detected at the anode and the DMPO/H and DMPO/D adducts were detected at both the anode and the cathode.[6b] These results were interpreted in terms of crossover processes: of O_2 from the cathode to the anode, thus explaining the formation of the DMPO/OOH adduct at the cathode and of H_2 and D_2 from the anode to the cathode, thus explaining the presence of DMPO/H and DMPO/D at the cathode. The results have suggested that, in a membrane electrode assembly (MEA), the hydrogen atoms are formed at the Pt catalyst site: At the anode catalyst from the fuel and at the cathode catalyst from crossover hydrogen. Taken together, these studies have formulated *three* degradation paths for the PEMs: main chain unzipping, side chain attack (both by attack of hydroxyl radicals), and main and side chain scission by hydrogen atoms.[4,6] Main chain unzipping and side chain attack have received additional support from studies that used different methods, for example, fluoride ion emission rate, FTIR, ^{19}F NMR, and liquid chromatography−mass spectroscopy.[5,7]

Recent results have suggested that in a FC the Pt catalyst is present not only at the anode and cathode sides of the MEA, but also *inside* the membrane:[8] At high potential and low pH conditions, Pt dissolves from the cathode and can migrate through the membrane. In contact with hydrogen, Pt precipitates throughout the membrane and forms a Pt band. The location of the band depends on fuel cell operating conditions and is formed only after the first ≈50 h of FC operation at OCV conditions.[8a] Radicals generated *inside* the membrane due to the presence of the Pt band can then attack the polymer and lead to *local* membrane fragmentation.[9] Therefore, to fully understand the reactions between the $H^{\bullet}$ and $HO^{\bullet}$ aggressors and the membrane it is necessary to track stable degradation products generated *inside* the membrane: An *in-depth* analysis of the degradation products is a must.

In this Letter, we respond to the in-depth challenge by micro FTIR cross-sectional analysis of two Nafion 115 MEAs degraded during 52 or 180 h and at open-circuit voltage (OCV) conditions at 90 °C and 30% relative humidity. The 2D spectral-spatial maps generated in these experiments present the variation of the FTIR bands as a function of depth; provide information on the distribution of the functional groups along the MEA cross-section; and determine the location of membrane degradation products in the spatial dimension, from the cathode to the anode. Some micro FTIR techniques have been described in the literature.[10−14] To the best of our knowledge, we report here the first in-depth analysis of membrane fragmentation in a PEMFC and the first experimental evidence suggesting that membrane attack by $H^{\bullet}$, initiated at both the main chain and the side chain of the polymer, is an important step in the membrane degradation process.

Optical images of cross sections for nondegraded Nafion 115 membrane (thickness 125 μm) and for Nafion MEAs degraded during 52 and 180 h are shown in Figure 1.

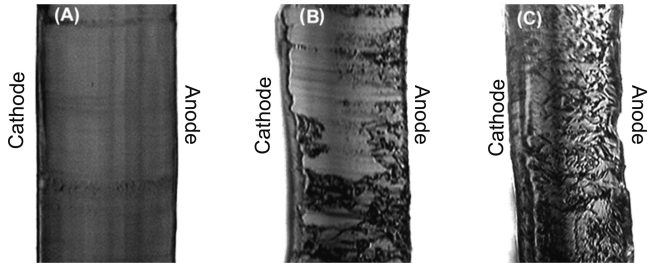

Figure 1. Optical images of microtomed cross sections for Nafion membranes after removal of the catalyst layer: nondegraded (A), degraded for 52 h (B), and degraded for 180 h (C) at open circuit voltage (OCV) conditions, 90 °C, and 30% relative humidity. Images of degraded MEAs were collected with the optical camera of the Perkin-Elmer Spotlight 200 microscope system after removal of the catalyst layer. The dark shading in (C) is due to the microscope light source. The optical images are shown in two spatial dimensions. Additional experimental details are in the Supporting Information

Images B and C of Figure 1 show highly degraded loci in the Nafion MEAs; it is clear that the extent of degradation and the location of degraded areas are inhomogeneously distributed and strongly dependent on the degradation time. The highly degraded membrane is thinner in some spots, as seen in Figure 1C. The presence of pinholes, fractures in, and thinning of the membranes after PMCFC operation has been reported and can lead to mechanical and chemical failure of the membrane.[15]

The line scan maps of Nafion membranes, nondegraded and degraded during 52 and 180 h, are presented in Figure 2. Degradation of Nafion has been investigated by FTIR spectroscopy and DFT studies of model compounds that mimic the polymer side chain helped in the understanding of the fingerprint region of IR spectrum.[16] The band assignments presented here are based on data available in the literature. Weak and broad bands at 3212 and 1750 cm^{-1} are expected due to the presence of water on the surface of the membrane. However, in the FTIR spectra collected here in reflectance mode, these bands have a very low intensity compared to the ATR-FTIR spectra collected in the transmittance mode, because the water content on the surface of the membrane is much lower compared to bulk. Bands at 1328 and 1310 cm^{-1} in Figure 2A−C are due to asymmetric vibrations of CF_3 and SO_3^- groups, respectively. The region between 1300 and 1100 cm^{-1} is completely obscured by the strong C−F absorptions. The strong band at 1248 cm^{-1} is due to the C−F vibrations in CF_2 groups. The strong and well separated band at 1156 cm^{-1}

dx.doi.org/10.1021/mz200100s | *ACS Macro Lett.* 2012, 1, 280−285

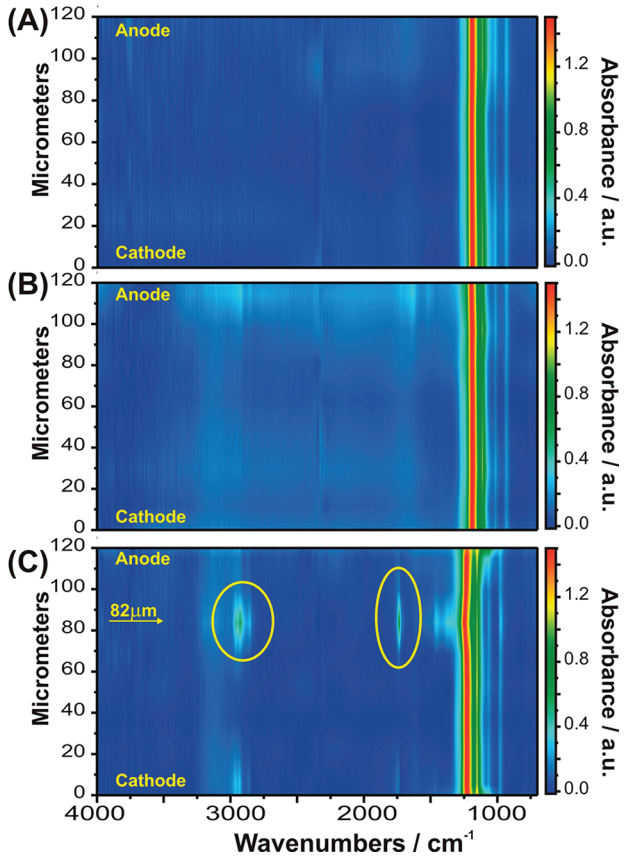

Figure 2. 2D spectral-spatial maps of Nafion 115 membrane: nondegraded (A), degraded during 52 h (B), and degraded during 180 h (C). Yellow ovals in (C) show the appearance of strong bands at a depth of 82 μm from the cathode as a result of membrane degradation. Weaker bands at the same frequency are also visible at 22 μm from the cathode. The acquisition time for each 2D spectral-spatial map was 150 min. Additional experimental details are in the Supporting Information.

is due to the asymmetric vibration of the C−O−C group. The band at 1064 cm^{-1} is assigned to SO_3 vibrations and is typical for the dissociated sulfonic group. Bands at 980 and 970 cm^{-1} can be assigned to the vibrations of $-CF_3$ and C−S groups in the side chain, respectively. ATR-FTIR spectra of membranes and model compounds, and DFT calculations published recently by us led to an understanding of the fingerprint region of membranes, including Nafion, and to a re-examination and reassignment of some bands presented in the literature for Nafion and Dow (Aquivion) membranes.[16d]

As seen in Figure 2B, degradation during 52 h leads only to small changes of band intensities. However, significant changes are seen in the 2D spectral map shown in Figure 2C, for Nafion MEA degraded for 180 h. Compared with the nondegraded membrane and membrane degraded for 52 h (Figure 2A and B, respectively), relatively strong bands around ≈2930 and 1740 cm^{-1} are observed near the anode at a depth of 82 μm from the cathode; these bands are visible but weaker at 22 μm from the cathode.

The FTIR spectra of Nafion MEAs extracted from the spectral maps shown in Figure 2 are presented in Figure 3 as a function of depth for the three membranes: nondegraded (A) and degraded during 52 h (B) and 180 h (C). The bottom spectra in Figure 3A and B correspond to the cathode side. In Figure 3C, the bottom spectrum was collected at 7 μm from the cathode, because the membrane lost some thickness during degradation.

Data presented in Figures 2 and 3 are for the selected cross-section; other cross-sections were also examined, and the corresponding degradation bands were more, or less, pronounced, as expected from the spatially heterogeneous membrane degradation shown in Figure 1.

As shown in Figure 3, the FTIR spectra of a nondegraded Nafion membrane and one degraded for 52 h do not change with depth. In the membrane degraded for 180 h, the intensities of the absorption bands assigned to C═O and C−H vary through the membrane cross-section and appear with maximum intensity at a depth of 82 μm from the cathode. Comparison of the FTIR spectrum recorded at 82 μm from the

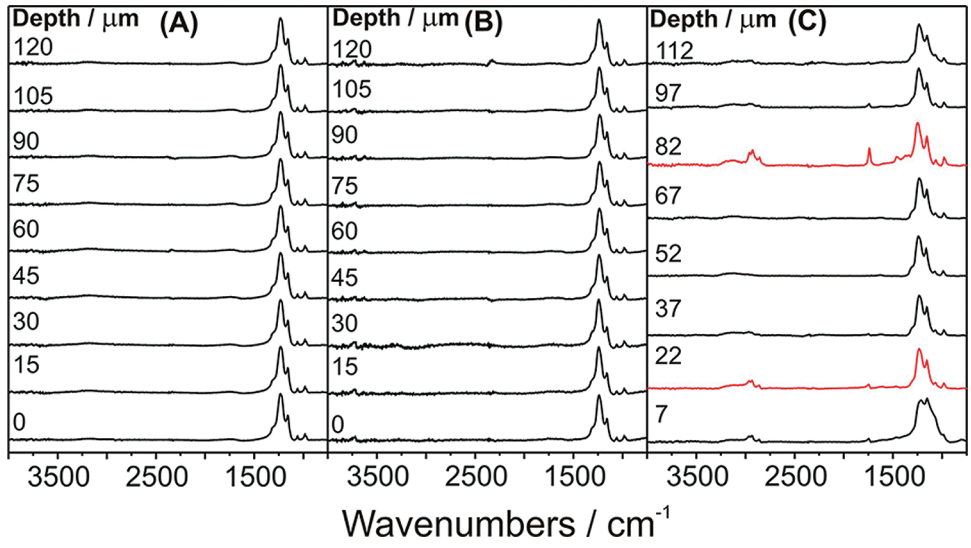

Figure 3. In-depth profiling: FTIR spectra of the Nafion 115 membrane as a function of depth from the cathode: nondegraded membrane (A), degraded for 52 h (B), and degraded for 180 h (C). In (C), spectra in red show the highest intensities of degradation species: at 82 and 22 μm from the cathode. All spectra were recorded in reflectance mode with the Perkin-Elmer Spotlight 200 microscope system.

dx.doi.org/10.1021/mz200100s | ACS Macro Lett. 2012, 1, 280−285

cathode with a spectrum of a nondegraded Nafion membrane is presented in Figure 4. Bands at 3120, 2962, 2928, and 2356

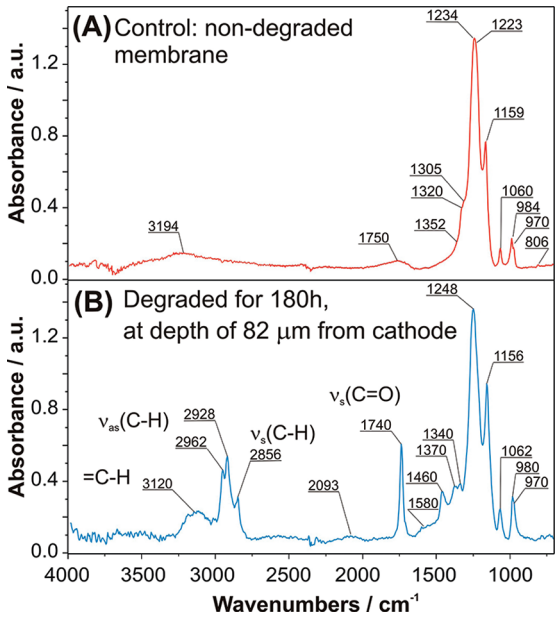

Figure 4. Comparison of the FTIR spectra of nondegraded Nafion 115 MEA (A) with the FTIR spectrum recorded at a depth of 82 μm for the membrane degraded during 180 h (B).

cm^{-1} are associated with C−H vibrations, and the strong band at 1740 cm^{-1} is assigned to the stretch mode of the C═O group.

The intensity variation of the degradation bands, C−H and C═O, with the distance from the cathode, for the MEA degraded during 180 h is shown in Figure 5.

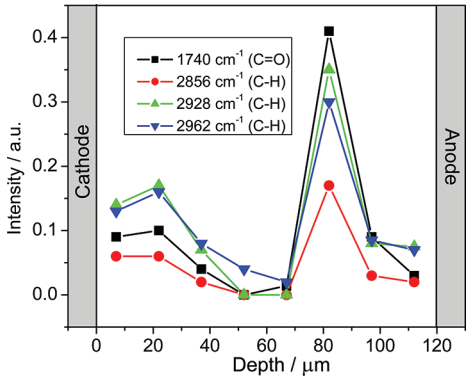

Figure 5. The intensity variation of the C−H and C═O absorption bands as a function of depth from the cathode for the MEA degraded during 180 h. The band at 1740 cm^{-1} corresponds to the vibration of C═O group, and bands at 2856, 2928, and 2962 cm^{-1} are due to C−H vibrations. Cathode and anode sides are indicated by gray bars.

The degradation bands have intensity maxima at the same depths, 22 and 82 μm. The C═O band can be generated by attack of hydroxyl radicals on the −COOH groups at chain ends, as described in the unzipping mechanism.[3] However, this mechanism will not increase the number of carboxylic groups which, as seen in Figure 3A, is initially very low. The C═O band intensity generated by degradation is significantly higher, as clearly seen in Figure 3C, for the membrane degraded during 180 h. The increase in the intensity of the C═O band must be the result of another degradation pathway, most likely from the radical attack on the side chain. Indeed, oxygen-centered radicals have been detected as spin adducts during the degradation of model compounds for the Nafion side chain.[17] However, we have to consider the results in Figure 5, which clearly show that the degradation bands C═O and C−H appear *at the same depths*, suggesting their generation by the same degradation mechanism. We propose that the presence of both bands is a result of a very important first step: abstraction of a fluorine atom from the Nafion main chain and side chain by $H^{\bullet}$, as shown in Scheme 1 for abstraction from the tertiary carbon atoms;[18,19] this process is expected to lead to scission of the main chain and of the side chain and to the generation of C═O and $R_F-CF_2^{\bullet}$ radicals. A similar pathway has been proposed by Coms.[18]

The $R_F-CF_2^{\bullet}$ radicals can react further, as shown in reactions 1−4 below, leading to the formation of the C−H and C═O groups detected in this study.

$$R_F-CF_2^{\bullet} + H_2O_2 \rightarrow R_F-CF_2H + HOO^{\bullet} \quad (1)$$

$$R_F-CF_2^{\bullet} + H_2O_2 \rightarrow R_F-CF_2OH + HO^{\bullet} \quad (2)$$

$$R_F-CF_2OH + H_2O \rightarrow R_F-CO_2H + 2HF \quad (3)$$

$$R_F-CF_2^{\bullet} + H_2 \rightarrow R_F-CF_2H + H^{\bullet} \quad (4)$$

The results presented in this study illuminate the major difference between ex situ experiments performed on model compounds (MCs) for the ionomer membranes and in situ experiments in an operating PEMFC: The ex situ studies are performed in the presence of hydroxyl radicals, $HO^{\bullet}$, which are considered major aggressors of the PEM and of the MCs. The situation in a PEMFC is, however, more complicated: The membrane is subjected not only to hydroxyl radicals, but also to $H^{\bullet}$ radicals.[6b] We anticipate that ex situ experiments performed in the presence of $HO^{\bullet}$ *and* $H^{\bullet}$ radicals be more representative of reactions in a FC.

The increased degradation in the anode area indicated in the in-depth analysis presented here is in accord with a scanning electron microscopy study of cross-sectional images of MEAs, which showed that the anode side is more degraded than the cathode in terms of membrane thinning.[20] The present results indicate, specifically, a maximum degree of degradation at 82 μm from the cathode in a Nafion membrane of thickness 125 μm.

Finally, the in-depth approach described above is expected to be generally applicable not only to membranes in FCs, but also to polymeric materials that degrade as a result of exposure to environmental factors, leading to a spatial variation of the extent of degradation that can be visualized by in-depth profiling using micro FTIR.

In this study we have presented a micro FTIR in-depth 2D profiling of cross sections for Nafion 115 membranes in MEAs degraded at open circuit conditions (OCV) for 52 or 180 h at 90 °C and 30% relative humidity. As a result of degradation, C═O and C−H bands appeared in the FTIR spectra. Cross-sectional line profile analysis of the MEA degraded for 180 h showed that the highest intensity of degradation bands is at a depth of 82 μm from the cathode. Weaker degradation bands were also observed, at a depth of 22 μm from the cathode. Degradation at these depths is most likely associated with the location of a Pt band formed after catalyst dissolution and Pt

dx.doi.org/10.1021/mz200100s | *ACS Macro Lett.* 2012, 1, 280−285

Scheme 1. Mechanism of H• Attack on the Nafion Main Chain and Side Chain and Generation of C═O Groups and R_F–CF_2• Radicals

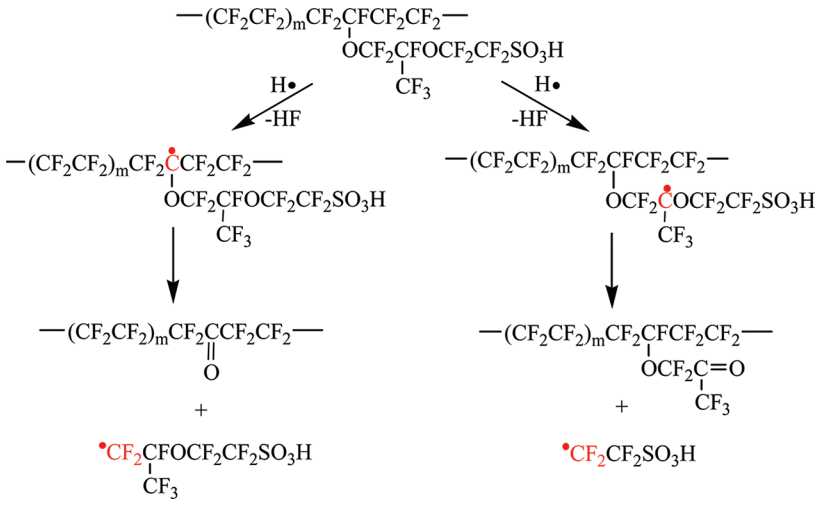

migration *inside the membrane*. Single frequency depth profiles of C═O and C–H vibrations showed that the anode side suffered more damage.

The appearance of the degradation bands, C═O and C–H, at the same depth strongly suggests that they are generated by the same mechanism. This result was rationalized by a very important first step: Abstraction of the fluorine atom from the main chain and in the side chain by hydrogen atoms, H•. This reaction is expected to cause main chain scission and to generate both –COOH groups and RCF_2H fragments.

The results presented in this study have shown that high spatial resolution techniques such as micro FTIR can provide valuable information on the location of membrane degradation sites, on the spatial distribution of functional groups over the degraded area, and on the mechanism of membrane degradation in operating fuel cells.

■ ASSOCIATED CONTENT

Supporting Information

Experimental details. This material is available free of charge via the Internet at http://pubs.acs.org.

■ AUTHOR INFORMATION

Corresponding Author

*Tel. 1-313-993-1012. Fax 1-313-993-1144. E-mail: schlicks@udmercy.edu.

Notes

The authors declare no competing financial interest.

‡On leave from the Faculty of Chemistry, Jagiellonian University, Ingardena 3, 30-060 Krakow, Poland.

■ ACKNOWLEDGMENTS

The development of the 2D spectral-spatial FTIR technique in our laboratories was supported by grants from the U.S. Department of Energy Cooperative Agreement No. DE-FG36-07GO17006, the Polymers Program of NSF, General Motors, and Ford Motor Co. DOE support does not constitute an endorsement by DOE of the views expressed in this publication. Illuminating discussions on membrane degradation with D. A. Schiraldi (Case Western Reserve University) and J. E. McGrath (Virginia Polytechnic Institute) are greatly appreciated.

■ REFERENCES

(1) Adzic, R. In *Electrocatalysis*; Lipkowski, J., Ed.; Wiley-VCH: New York, 1998; pp 197–242. (b) Mauritz, K. A.; Moore, R. B. *Chem. Rev.* **2004**, *104*, 4535–4585. (c) Roduner, E.; Schlick, S. In *Advanced ESR Methods in Polymer Research*; Schlick, S., Ed.; Wiley: Hoboken, NJ, 2006; Chapter 8, pp 197–228.

(2) (a) Borup, R.; Meyers, J.; Pivovar, B.; Kim, Y. S.; Mukundan, R.; Garland, N.; Myers, D.; Wilson, M.; Garzon, F.; Wood, D.; Zelenay, P.; More, K.; Stroh, K.; Zawodzinski, T.; Boncella, J.; McGrath, J. E.; Inaba, M.; Miyatake, K.; Hori, M.; Ota, K.; Ogumi, Z.; Miyata, S.; Nishikata, A.; Siroma, Z.; Uchimoto, Y.; Yasuda, K.; Kimijima, K.; Iwashita, N. *Chem. Rev.* **2007**, *107*, 3904–3951. (b) Endoh, E. *ECS Trans.* **2008**, *16*, 1229–1240. (c) Coms, F. D.; Liu, H.; Owejan, J. E. *ECS Trans.* **2008**, *16*, 1735–1747.

(3) (a) Curtin, D. E.; Lousenberg, R. D.; Henry, T. J.; Tangeman, P. C.; Tisack, M. E. *J. Power Sources* **2004**, *131*, 41–48. (b) Healy, J.; Hayden, C.; Xie, T.; Olson, K.; Waldo, R.; Brundage, A.; Gasteiger, H. A.; Abbott, J. *Fuel Cells* **2005**, *5*, 302–308.

(4) (a) Kadirov, M. K.; Bosnjakovic, A.; Schlick, S. *J. Phys. Chem. B* **2005**, *109*, 7664–7670. (b) Lund, A.; Macomber, L.; Danilczuk, M.; Stevens, J.; Schlick, S. *J. Phys. Chem. B* **2007**, *111*, 9484–9491.

(5) (a) Zhou, C.; Guerra, M. A.; Qiu, Z. M.; Zawodzinski, T.; Schiraldi, D. A. *Macromolecules* **2007**, *40*, 8695–8707. (b) Schiraldi, D. A.; Savant, D.; Zhou, C. *ECS Trans.* **2010**, *33*, 883–888.

(6) (a) Danilczuk, M.; Coms, F. D.; Schlick, S. *Fuel Cells* **2008**, *8*, 436–452. (b) Danilczuk, M.; Coms, F. D.; Schlick, S. *J. Phys. Chem. B* **2009**, *113*, 8031–8042. (c) Danilczuk, M.; Schlick, S.; Coms, F. D. *Macromolecules* **2009**, *42*, 8943–8949.

(7) Ghassemzadeh, L.; Kreuer, K. D.; Maier, J.; Muller, K. *J. Phys. Chem. C* **2010**, *114*, 14635–14645 and references therein.

(8) (a) Péron, J.; Nedellec, Y.; Jones, D. J.; Rozière, J. *J. Power Sources* **2008**, *185*, 1209–1217. (b) Inaba, M. *ECS Trans.* **2009**, *25*, 573–581.

(9) (a) Haugen, G.; Barta, S.; Emery, M.; Hamrock, S.; Yandrasits, M. In *Fuel Cell Chemistry and Operation*; Herring, A.M, Zawodzinski, T.A., Jr., Hamrock, S.J., Eds.; American Chemical Society: Washington, DC, 2010; pp 137–151. (b) Madden, T.; Weiss, D.; Cipollini, N. E.; Condit, D.; Gummalla, M.; Burlatsky, S.; Atrazhev, V. *J. Electrochem. Soc.* **2009**, *156*, B657–B662. (c) Yoon, W.; Huang, X. *J. Electrochem. Soc.* **2010**, *157*, B599–B606. (d) Mittal, V. O.; Kunz, H. R.; Fenton, J. M. *J. Electrochem. Soc.* **2007**, *154*, B652–B656.

(10) Okumura, H.; Takahagi, T.; Nagai, N.; Shingubara, S. *J. Polym. Sci., Part B: Polym. Phys.* **2003**, *41*, 2071–2078.

(11) Gu, X.; Michaels, C.; Drzal, P.; Jasmin, J.; Martin, D.; Nguyen, T.; Martin, J. *J. Coat. Technol. Res.* **2007**, *4*, 389–399.

(12) Nagai, N.; Matsunobe, T.; Imai, T. *Polym. Degrad. Stab.* **2005**, *88*, 224–233.

(13) Nagle, D. J.; George, G. A.; Rintoul, L.; Fredericks, P. M. *Vibr. Spectrosc.* **2010**, *53*, 24−27.
(14) Mahdavi, H.; Sadeghzadeh, B. O. *J. Polym. Sci., Part B: Polym. Phys.* **2010**, *48*, 356−363.
(15) Gittleman, C. S.; Coms, F. D.; Lai, Y.-H. In *Modern Topics in Polymer Electrolyte Fuel Cell Degradation*; Mench, M., Kumbur, E. C., Veziroglu, T. N., Eds.; Elsevier: New York, 2012; pp 15−88.
(16) (a) Chen, C.; Levitin, G.; Hess, D. W.; Fuller, T. F. *J. Power Sources* **2007**, *169*, 288−295. (b) Warren, D. S.; McQuillan, A. J. *J. Phys. Chem. B* **2008**, *112*, 10535−10543. (c) Webber, M.; Dimakis, N.; Kumari, D.; Fuccillo, M.; Smotkin, E. S. *Macromolecules* **2010**, *43*, 5500−5502. (d) Danilczuk, M.; Lin, L.; Schlick, S.; Hamrock, S. J.; Schaberg, M. S. *J. Power Sources* **2011**, *196*, 8216−8224.
(17) Spulber, M.; Schlick, S. *J. Phys. Chem. B* **2011**, *115*, 12415−12421.
(18) Coms, F. D. *ECS Trans.* **2008**, *16*, 235−255.
(19) Yu, T. H.; Sha, Y.; Liu, W.-G.; Merinov, B. V.; Shirvanian, P.; Goddard, W. A. *J. Am. Chem. Soc.* **2011**, *133*, 19857−19863.
(20) Shim, J. Y.; Tsushima, S.; Hirai, S. *ECS Trans.* **2007**, *11*, 1151−1156.